Three Dimensional Transient Asymmetric Flowfields in Physical Vapor Transport

Joseph Dobmeier
Minnesota State University, Mankato

Three Dimensional Transient Asymmetric Flowfields in Physical Vapor Transport

Joseph Dobmeier, Minnesota State University, Mankato
Dr. Patrick Tebbe, Minnesota State University, Mankato

Abstract

Physical Vapor Transport is a manufacturing process used to produce single crystals of semiconductor materials such as mercurous chloride (Hg_2Cl_2). In the past this time-varying process has been studied with numerical simulation by considering three dimensional flow using an axi-symmetric two dimensional model or by restricting the simulation to asymmetric two dimensional flow and dropping the assumption of axi-symmetry from the model. It is generally agreed that neither of these methods accurately represent the true behavior of the process. The purpose of this research was to extend the asymmetric two dimensional model to three dimensions thereby obtaining a solution which more authentically characterizes reality. The resulting data was then visualized and analyzed. The simulations were performed with a commercially available computational fluid dynamics software package called FIDAP on the 140-processor "supercomputer" at Minnesota State University, Mankato. The visualization tool used was Tecplot 360. The results have shown that the flowfield is indeed asymmetric and cannot be accurately described by a two dimensional simplification.

Introduction

Fluorescence spectroscopy and robotic applications in the area of machine vision rely on a class of crystalline materials with unique acousto-optic properties. The materials respond to sound wave vibration by altering the amplitude and frequency of light passing through them. This property is useful for modulating the frequency of laser light and in constructing adjustable light filters. Mercurous Chloride (Hg_2Cl_2) is of particular interest because of its high efficiency in the long wavelength infrared region of the electromagnetic spectrum [1]. The devices require material with highly ordered and regular arrangements of atoms to function properly. One manufacturing process called Physical Vapor Transport (PVT) involves slowly growing low-defect crystalline materials by sublimating raw material to a vapor and condensing it on a deposition surface. The behavior of the flowing vapor has a large impact on the quality of the finished product. When the flowfield is steady and uniform the material is deposited in a desirably uniform way. If the flowfield never "settles down," the material is deposited haphazardly in a decidedly non-uniform manner. This causes some portions of the crystal to grow faster than others producing dislocations in the crystal structure thus lowering quality.

The mathematic description of the system is such that a satisfactory analytical solution is not attainable. For this reason computer simulation has been identified as an appropriate technique

for predicting how a given set of physical parameters will affect the flowfield. Unfortunately, engineers historically have not been able to adequately optimize this process due to the overwhelming computational requirements. Often the problem is approximated as two-dimensional (2D) and steady in time [2-5]. However, computer abilities are now starting to reach the point where 3D, transient simulation is becoming feasible.

The purpose of this research was to extend the 2D model (constructed by Tebbe [2]) into 3D, providing a link between past research and future experiments. First, the mathematic description of the system will be explained. Second, the solution methodology will be described. Next, results will be presented. Then, similarities to and differences from 2D simulations will be discussed followed by plans for future research.

Mathematic Description

Solute material Hg_2Cl_2 first sublimes from the heated floor of a cylindrical cavity (source). It then undergoes vapor transport through an inert atmosphere before being deposited through condensation on the cooled ceiling (crystal). The system is described by a series of coupled partial differential equations. The equations correspond to the Navier-Stokes laws of continuity, conservation of momentum, conservation of energy and conservation of the solute material (Eqs. (1) - (4)). Velocity at any point was taken to be the mass average of the solute and inert gas velocities at that point. Total pressure was assumed constant.

$$\nabla \cdot \vec{u} = 0 \tag{1}$$

$$\rho_0 \left(\frac{\partial \vec{u}}{\partial t} + \vec{u} \cdot \nabla \vec{u} \right) = -\nabla p + \mu \nabla^3 \vec{u} + \rho n \vec{g_0} \tag{2}$$

$$\rho_0 \left(\frac{\partial T}{\partial t} + \vec{u} \cdot \nabla T \right) = \nabla \cdot (k \nabla T) \tag{3}$$

$$\rho_0 \left(\frac{\partial \omega}{\partial t} + \vec{u} \cdot \nabla \omega \right) = \rho_0 \nabla \cdot (D_{AB} \nabla \omega) \tag{4}$$

A Boussinesq approximation (Eq. 5) was used to estimate the effect of temperature and solute concentration on density

$$\rho = \rho_0 (1 - \beta \Delta T - \gamma \Delta \omega) \tag{5}$$

where

$$\beta = -\frac{1}{\rho} \frac{\partial \rho}{\partial T} \bigg)_{p*,\, \omega_A^*}$$

$$\gamma = \frac{1}{\rho} \frac{\partial \rho}{\partial \omega} \bigg)_{p*,\, T^*}$$

Because of the low temperature differences between the source and crystal, material properties were assumed constant.

Boundary conditions:

The walls of the chamber were assumed to be adiabatic, impermeable and no slip (i.e. tangential velocity is zero). The tangential components of the velocity at the source and crystal were set to zero. The normal components of the velocity were derived from the sublimation/condensation mass flux at the boundaries using Dalton's law of partial pressures (6a) and (6b). The temperatures of the source and crystal were fixed.

$$v_s = -\frac{D_{AB}}{1-\omega_s}\frac{\partial\omega}{\partial y}\bigg|_s \qquad (6a)$$

$$v_c = -\frac{D_{AB}}{1-\omega_c}\frac{\partial\omega}{\partial y}\bigg|_c \qquad (6b)$$

Initial conditions:

Initial velocities were set at zero while temperature and concentration were initialized to linear profiles.

Scaling:

The variables were converted to non-dimensional format using the following scaling factors:

$$x^* = \frac{x}{D},\ y^* = \frac{y}{H},\ z^* = \frac{z}{D},\ u^* = \frac{v}{U_c},\ v^* = \frac{v}{U_c},\ w^* = \frac{w}{U_c},\ t^* = \frac{t}{T_t},\ \omega^* = \frac{\omega-\omega_c}{\Delta\omega},$$

$$T^* = \frac{T-T_c}{\Delta T},\ T_t = \frac{H^2}{\alpha},\ U_c = \frac{\alpha}{H},\ \Delta T = T_s - T_c,\ \Delta\omega = \omega_s - \omega_c$$

Six dimensionless parameters are of interest in this problem. They are the thermal Rayleigh number (Ra_t), Prandtl number (Pr), Lewis number (Le), Peclet number (Pe), concentration parameter (C_v) and aspect ratio (Ar). For this geometry, $D=H=5$cm resulting in an aspect ratio of unity. The rest of the parameters are defined as follows:

$$Ra_t = \frac{\beta\,\Delta T n\,g_0 H^3}{\bar{v}\alpha},\ Pr = \frac{\bar{v}}{\alpha},\ Le = \frac{\alpha}{D_{AB}},$$

$$Pe = \frac{U_0 H}{D_{AB}},\ C_v = \frac{1-\omega_c}{\Delta\omega},\ Ar = \frac{H}{D}$$

The thermal Rayleigh number is defined as the product of the Grashof and Prandtl numbers. The Grashof and Prandtl numbers describe the strength of the buoyancy forces and the ratio of thermal diffusivity to kinematic viscosity, respectively [6]. Note the two characteristic velocities (U_c and U_0) correspond to the characteristic velocity for natural convection and the streaming velocity which results from the sublimation/condensation advective-diffusive flux. Gravitational acceleration on the surface of the earth ($\overrightarrow{g_0}$) was supplied with a coefficient, n, to study the

stabilizing effect of a reduction in convective circulation as is experienced in the micro-gravity environment of orbiting laboratories. A series of seven cases were selected from Tebbe and Duval to provide a means of verification and validation (Table 1).

Table 1 - PVT physical parameters, $T_s = 330^{\circ}\text{C}$.

Case	ΔT (K)	n	Ra_t	Pr	Le	Pe	C_v	time step Δt^*
1	2	1	3.83×10^4	0.871	0.411	0.876	1.71	0.00125
2	7.5	1	1.80×10^5	0.831	0.366	1.90	1.28	0.00125
3	20	1	8.19×10^5	0.758	0.500	2.96	1.06	0.000125
4	30	1	1.92×10^6	0.717	0.540	3.50	1.03	0.000125
5	7.5	0.01	1.80×10^3	0.831	0.366	1.90	1.28	0.00125
6	7.5	0.001	1.80×10^2	0.831	0.366	1.90	1.28	0.00125
7	7.5	0.0001	1.80×10^1	0.831	0.366	1.90	1.28	0.00125

Methodology

FIDAP, a commercially available computational fluid dynamics package produced by Fluent Inc. was used to perform a Galerkin finite element solution of the simulation parameters. The boundary condition for velocity at the source and crystal required that a user-defined subroutine be called at each timestep for every node along the boundaries. The subroutine uses the nodal mass fraction from the previous iteration to perform a first-order estimate of the derivative of the mass fraction required by Eqs. 6a and 6b. Unfortunately, this method causes the flowrate between the source and crystal to violate continuity (Eq. 1). To work around this problem, an average value is computed for the source and crystal flowrates and a scaling factor is applied to boundary node velocities, thus satisfying the constraint. According to Tebbe, this method does not significantly alter flow structure development. The results of the simulations were converted to a neutral file format and imported into Tecplot 360, a 3D visualization program. Tecplot was used to create three types of plots: stream traces which characterize the main flow features, species concentration contour plots showing the distribution of vaporized Hg_2Cl_2 and the time history of solution variables at specific points.

Results

For case 1, normal gravity and a small temperature difference were considered. The flow structure began as a plume (Figure 1) but developed into a unicellular pattern (as in Figure 2) for dimensionless time greater than 0.07. Plume development and destabilization corresponds to the peak in the velocity magnitude dimensionless time history plot (Figure 4, case 1). The beginnings of the transition may be seen in Figure 1 as the helical streams move clockwise about the z-axis. This motion eventually disrupts the plume leading to the onset of the unicellular pattern which then approaches steady state.

Case 2 is normal gravity and a slightly higher temperature difference and displays the same evolution as case 1; but, the plume achieves much higher velocity than in case 1. The plume is destabilized before dimensionless time reaches 0.25. The helical streams then oscillate within the center of the cell as shown in Figure 4 for case 2.

Case 3 has normal gravity and one of the higher temperature differences of the simulations performed. Upon observation of the time history for velocity magnitude (Figure 4, case 3), there is no approach to steady state; indeed, the flow displays complex oscillatory behavior. This is also true of case 4.

As can be seen in Figure 3, reduced gravity case 5 is highly stabilized. Steady state is reached very quickly (dimensionless time approximately 0.15 from Figure 4, case 5) and results in uniform concentration gradients. Cases 6 and 7 were nearly identical to case 5.

Comparison with 2D Research

Case 1 deviates markedly from its 2D counterpart. In 2D there was no flowfield evolution past the initial plume; certainly there was no development of a unicellular roll. The implication is that $Ra_t = 3.83 \times 10^4$ is above the critical Rayleigh number (i.e. the Rayleigh number just high enough to produce a unicellular structure but below which a unicellular structure does not develop).

The single roll structure found in the 3D simulation of case 2 (Figure 2) agrees well with that displayed by the work of Tebbe and Duval; in addition, the species concentration contours are very similar. An aspect of the flowfield not captured by the 2D idealizations is the helical stream traces which begin at the bottom right of Figure 2 and wind through the center of the unicellular structure. The helical streams at the center of the roll do not reach steady state as is evident from the velocity magnitude dimensionless time history plot for case 2 in Figure 4. This is in contradiction to 2D solutions and suggests that the critical Rayleigh number for oscillation is smaller than indicated by 2D research.

For the reduced gravity cases 5-7 there were no significant behavioral differences between 2D and 3D. Both simulations predicted a roughly axi-symmetric parabolic flowfield as shown in Figure 3.

Plans for Future Research

In the immediate future the 3D results will be further analyzed for their transient characteristics. Specifically, phase-space analysis [7] will be applied to both the transient and oscillatory regions of the solution domains. Oscillations will also be analyzed using Fourier transformation to obtain their power spectrums in the frequency domain. Moving forward, more complicated geometries which accurately depict actual manufacturing processes will be subjected to the same solution and analysis sequence.

Nomenclature

2D	two dimensional
3D	three dimensional
Ar	aspect ratio
C_v	concentration parameter
D	cavity diameter
D_{AB}	molecular mass diffusion coefficient
$\vec{g_0}$	acceleration due to gravity on earth in the negative z-direction
H	cavity height
Le	Lewis number
n	ratio denoting modification of acceleration due to gravity
p	hydrodynamic pressure
Pe	Peclet number based on mass diffusion
Pr	Prandtl number
Ra_t	thermal Rayleigh number
t	dimensionless time
T	dimensionless temperature
T_t	characteristic time
u, v, w	dimensionless velocity in x-, y- and z-directions
U_c	characteristic velocity based on convection
U_0	characteristic velocity based on the advective-diffusive flux
x, y, z	dimensionless horizontal and vertical directions

Greek characters:

α	thermal expansion coefficient
β	thermal expansivity
Δ	difference
γ	solutal expansivity
μ	dynamic viscosity
ν	kinematic viscosity
ω	mass fraction
∇	gradient in the x-, y- and z-directions
ρ	density
∇^3	Laplacian in three directions

Subscripts:

c	crystal
s	source

Superscripts:

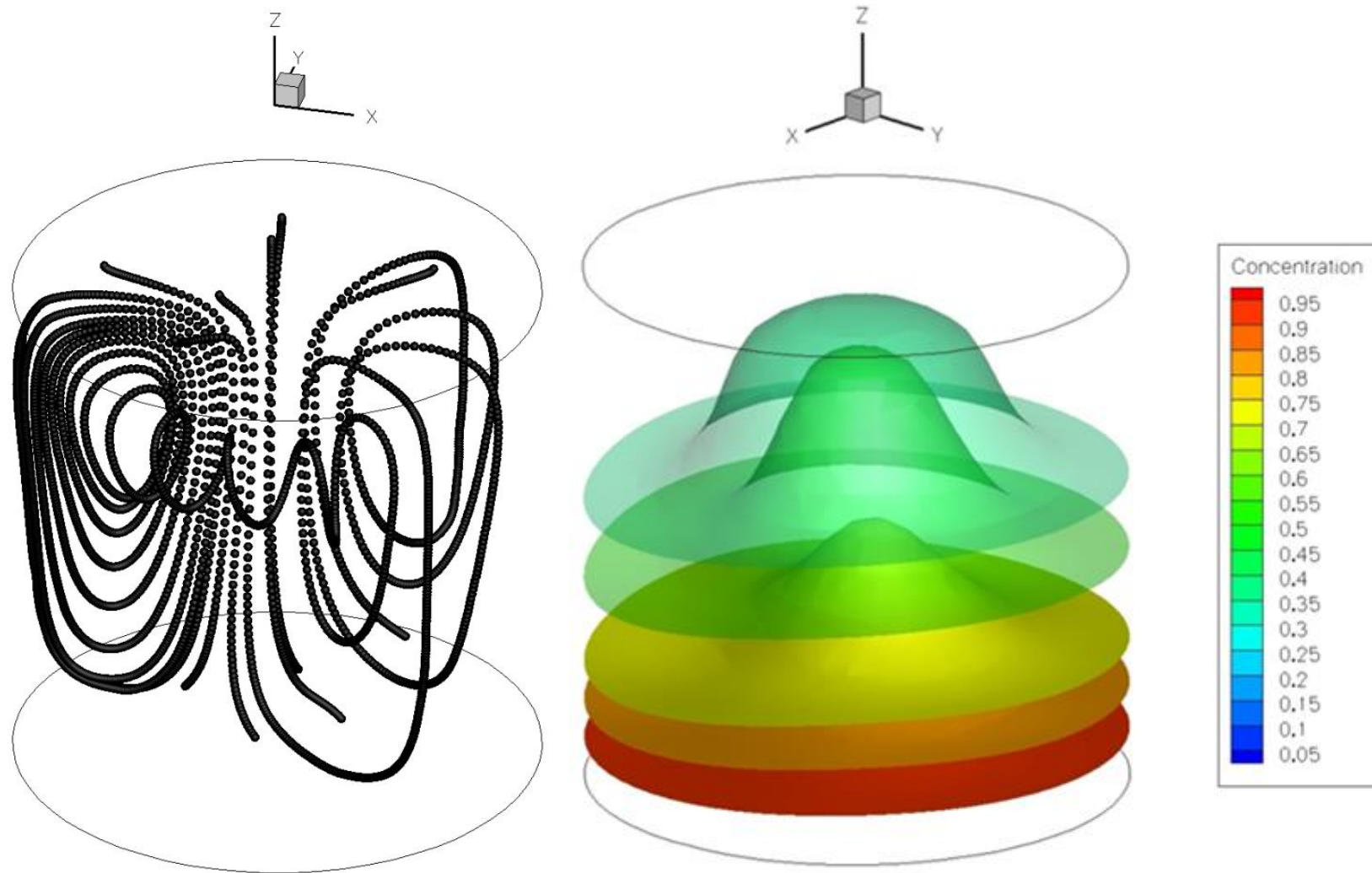|	
$*$	dimensionless quantity
$-$	average quantity

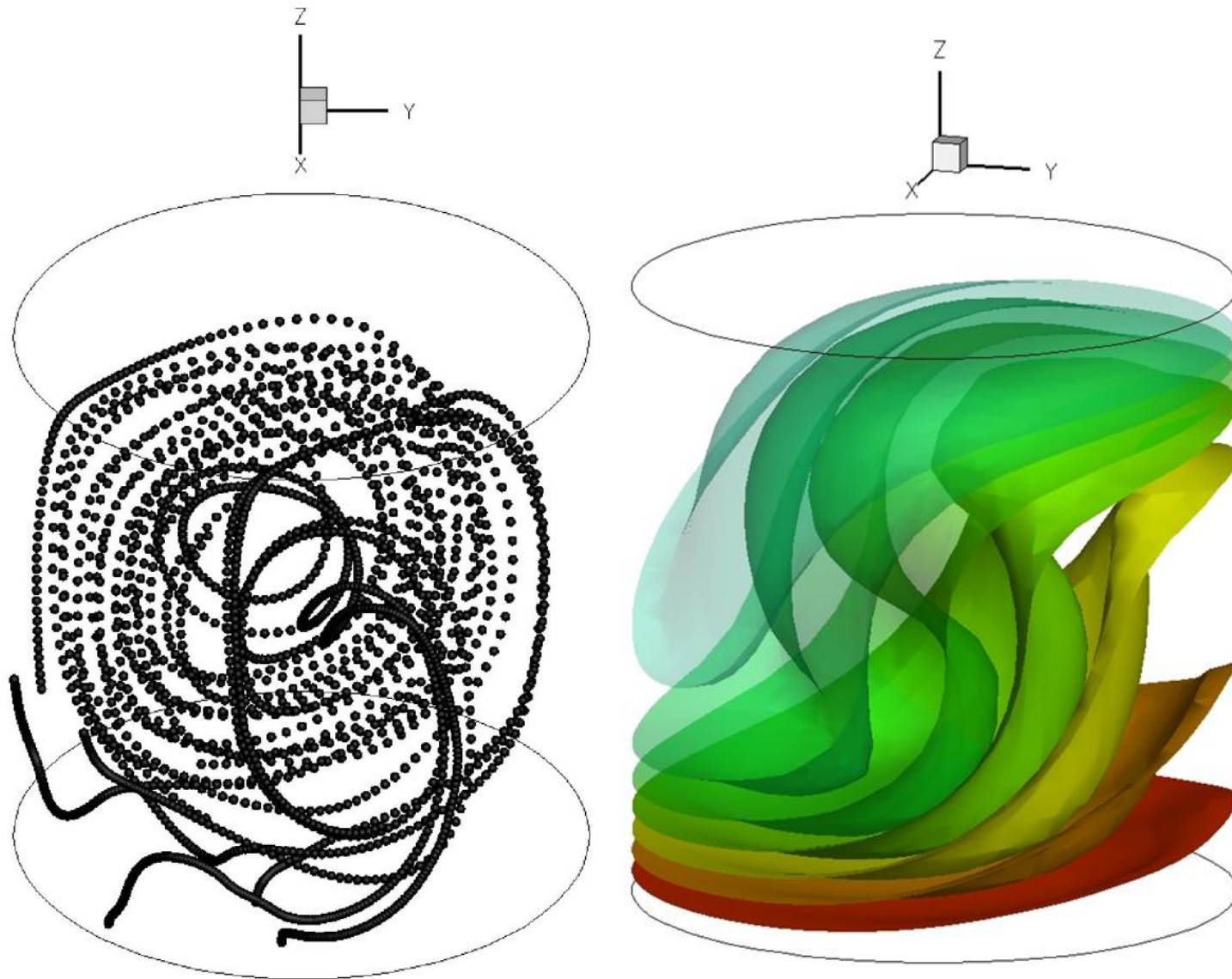**Figure 1 – Case 1 stream traces and concentration contours at time = 0.0675.**

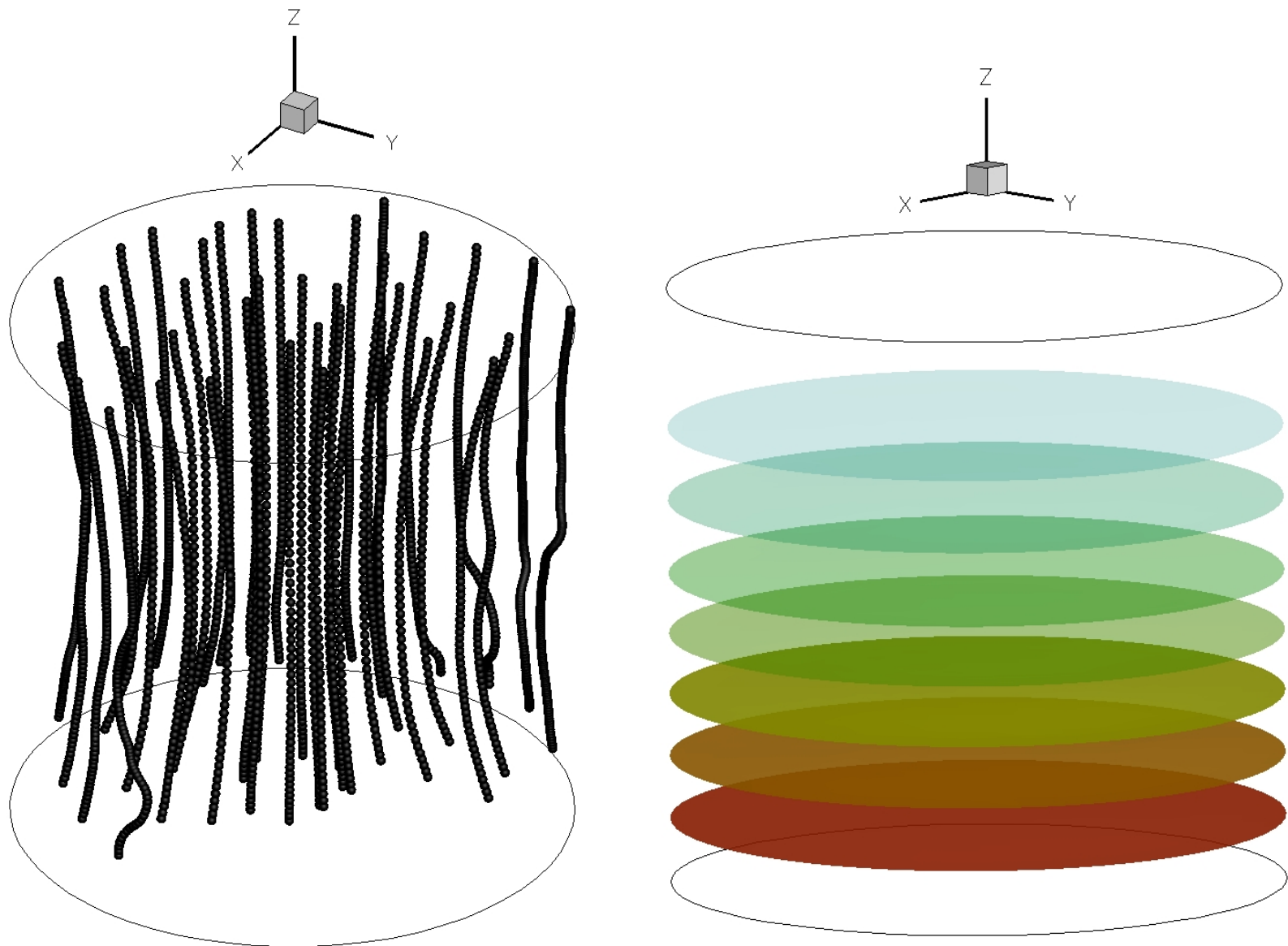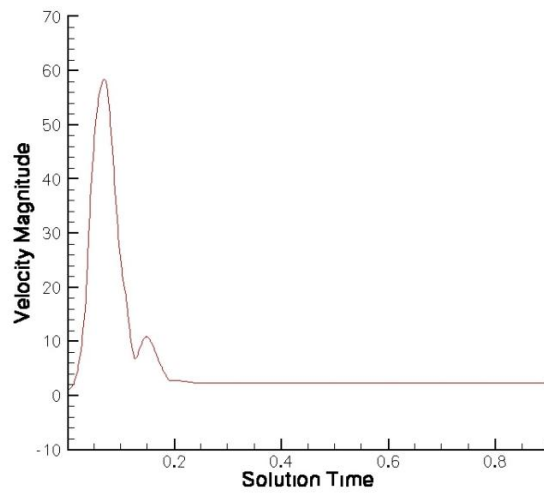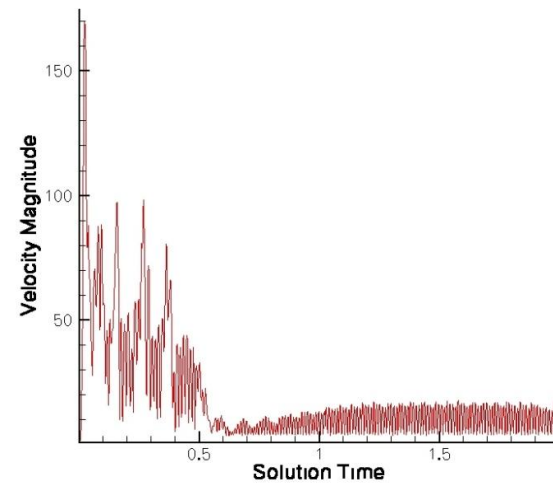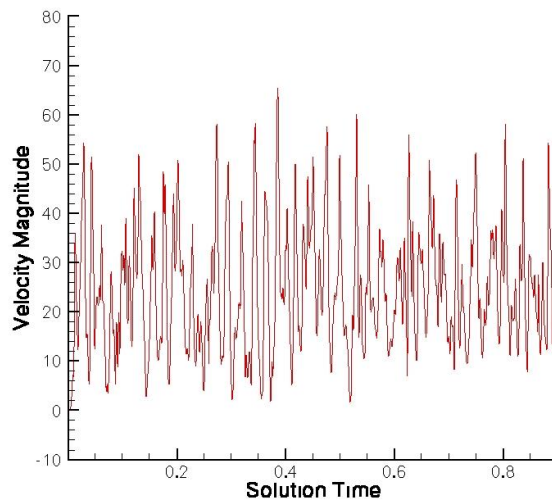**Figure 2 - Case 2 stream traces and concentration contours at time = 0.6025.**

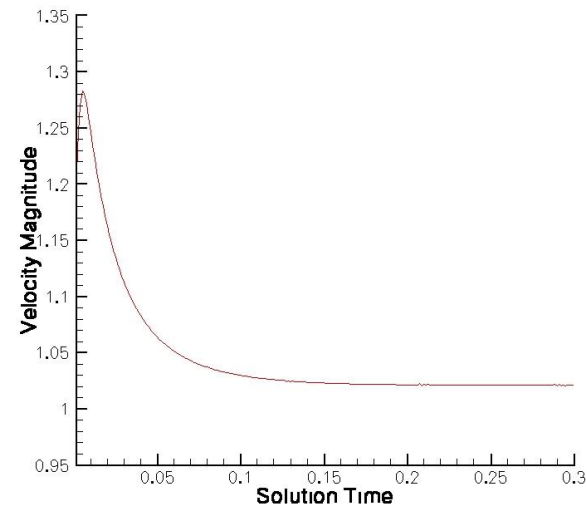**Figure 3 - Case 5 stream traces and concentration contours at time = 0.02625.**

Figure 4 - Velocity magnitude dimensionless time histories for selected cases at specified locations.

Bibliography

[1] Joo-Soo Kima, Sudhir B. Trivedia, Jolanta Soosa, Neelam Guptab, Witold Palosza. Growth of Hg_2Cl_2 and Hg_2Br_2 single crystals by physical vapor transport. Journal of Crystal Growth 310 (2008) 2457–2463.

[2] P. A. Tebbe, S.K. Loyalka, W. M. B. Duval. Finite element modeling of asymmetric and transient flowfields during physical vapor transport. Finite Elements in Analysis and Design 40 (2004) 1499-1519.

[3] W. M. B. Duval, Convection in the physical vapor transport process-I: thermal, J. Chem. Vapor Deposition 2 (1994) 188-217.

[4] W. M. B. Duval, Convection in the physical vapor transport process-II: thermosolutal, J. Chem. Vapor Deposition 2 (1994) 282-311.

[5] D. W.Greenwell, B. L. Markham and F. Rosenberger. Numerical modeling of diffusive physical vapor transport in cylindrical ampoules, Journal of Crystal Growth, 51 (1981) 413-425.

[6] R. B. Bird, W.E Stewart and E. M. Lightfoot. Transport Phenomena 2nd Ed., John Wiley & Sons Inc., (2002) 268, 353-356.

[7] F.C. Moon. Chaotic and Fractal Dynamics. John Wiley & Sons Inc., (1992) 53-55.

Joseph Dobmeier is a senior double-majoring in Mechanical Engineering and Computer Science with a minor in Mathematics at Minnesota State University, Mankato. During his enrollment at MSU, Mankato, he has been involved with the student chapter of the American Society of Mechanical Engineers (ASME) and Students for Sustainability club. From fall 2007 through spring 2009 he was a member of a team with four other students competing in the EPA-sponsored "Student Sustainable Design Competition." His team undertook the design, construction and testing of three prototype solar water heaters made from reclaimed or recycled materials and developed a mathematical model to predict their performance. Since 2006 he has been employed at MSU with Student Support Services providing individual math and science tutoring for disadvantaged students as well as entry-level training for new tutors. In 2008 he was hired to assist with research activities within the Department of Mechanical Engineering, leading to internships during the summers of 2008 and 2009. The internships were focused on providing programming support and engineering analysis for a variety of research projects. After graduation in May 2010, he hopes obtain employment in industry while also studying part-time for a graduate degree in Scientific Computing.